(GRIN) lens with a pitch of λ/4 and planoconvex lens (f = 3.5cm) were used to collimate the output beam and then focus the light to a spot on the sample surface.

In the present scheme differential photodetection of the reflected signal has been incorporated. Such a scheme can reduce common-mode noise, arising from intensity fluctuations of the probe laser beam. In our experiments specularly reflected light from the sensing position was directed into a polymer fibre-optic bundle (Toray Industries) consisting of 32 fibres. These fibres were split into two bundles of 16 fibres, leading to two high-speed *pin* photodetectors PD1 and PD2. The variation in light intensity, due to any lateral movement of the probe beam, was monitored across the bundle tip by differential photodetection. The use of an optical fibre bundle removed the strict geometrical constraints imposed by the knife edge approach whilst retaining the advantages of differential photodetection. The difference signal of the two photodiodes was amplified by a 40dB Analog Modules preamplifier with a 30MHz bandwidth. This signal was recorded by a Tektronix (TD5 520) 50MHz bandwidth digitising oscilloscope. Waveforms were subsequently captured on a 286 PC using LabWindows software for data acquisition and signal processing.

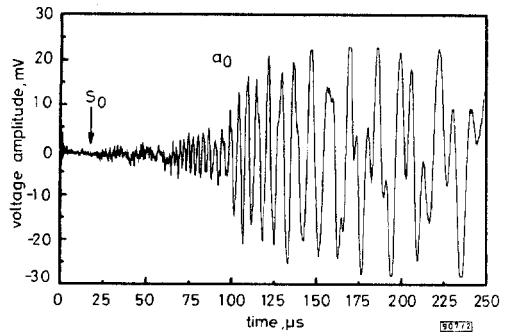

Fig. 2 *Thermoelastically generated Lamb waves in a 50μm-thick aluminium sheet*

Results: Results in Fig. 2 illustrate a transient Lamb wave acquired from a mechanically polished 50μm aluminium sheet by the differential fibre sensing device. Timing events were initiated at t = 0 from a fraction of the Nd:YAG laser used to trigger the oscilloscope. The Lamb waves were thermoelastically generated with the laser line source measuring 1.5mm in width and 2cm in length. Source-to-detector separation and probe beam spot diameter were measured as 62mm and 100μm, respectively. One can just discern the low-amplitude symmetric s_0 mode arrival followed by the frequency-dispersive a_0 mode. After 150μs, Lamb wave edge reflections and higher-order propagating modes are superimposed on the a_0 mode. The out-of-plane asymmetric Lamb wave amplitudes were estimated from Fig. 2 to reach 10nm with a signal/noise ratio of about 90:1.

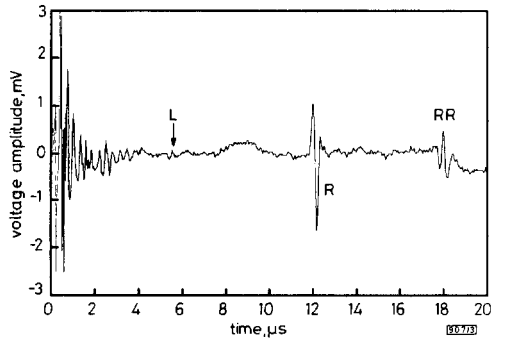

Fig. 3 *Thermoelastically generated longitudinal (L) and Rayleigh (R) waves in a 30mm aluminium block*

Waveform is average of 36 laser shots

This sensitivity is sufficient for the detection of elastic waves reflected from defects. As an example, a preliminary test of the optical system was conducted to detect elastic waves reflected from a surface-breaking slot. The experimental geometry used has been described elsewhere [5]. A 30mm-thick aluminium plate was subjected to both the thermoelastic laser pulse and probe laser beam. A 0.3mm-deep, 0.25mm-wide artificial defect was milled in the sample surface. The Nd:YAG line width was measured as 1.8 mm and its length as 2cm. The source-to-detector separation was 35.5mm and the defect-to-probe-beam separation was 9.5mm. Timing events were initiated at t = 0 with radio-frequency noise rapidly following from the firing of the laser. The transient ultrasound arising from 36 shots of the thermoelastic laser source is illustrated in Fig. 3. Although the signal/noise ratio is low, compared to the thermoelastically generated Lamb waves, distinct longitudinal (L) and Rayleigh (R) wave arrivals were observed. In addition, a signal corresponding to a Rayleigh wave component reflected from the defect (RR) was identified. This signal is similar to observations made by Cooper *et al.* and can be used to evaluate defect depth [5].

Conclusions: In summary, we have shown that laser-generated ultrasound can be measured with an all-optical fibre device based on the OBD technique. The fibre bundle incorporated differential photodetection to eliminate the requirement of a knife edge. The sensor system, with a 5mW He-Ne laser source, measured Lamb waves in thin, typically <425μm, metal sheet. It was also capable of measuring Rayleigh waves. Future work will be directed to the implementation of this device to quantitative NDT applications.

Acknowledgments: One of us (BAW) is grateful for a studentship awarded by the Engineering and Physical Sciences Research Council, United Kingdom. The research was partially funded under an EPSRC grant J30080.

11 January 1995
Electronics Letters Online No: 19950235

B.A. Williams and R.J. Dewhurst (*Department of Instrumentation and Analytical Science, UMIST, PO Box 88, Manchester M60 1QD, United Kingdom*)

References

1 DAVIES, S.J., EDWARDS, C., TAYLOR, G.S., and PALMER, S.B.: 'Laser-generated ultrasound: Its properties, mechanisms and multifarious applications', *J. Appl. D.: Appl. Phys.*, 1993, **26**, pp. 329–348
2 MONCHALIN, J.P.: 'Optical detection of ultrasound', *IEEE Trans.*, 1986, **UFFC-33**, pp. 485–499
3 DEWHURST, R.J., NOUI, L., and SHAN, Q.: 'Polymer film thickness measurement using laser-ultrasound techniques', *Rev. Sci. Instrum.*, 1990, **61**, pp. 1736–1742
4 SCRUBY, C.B., and DRAIN, L.E.: 'Laser ultrasonics: techniques and appplications' (Adam Hilger, 1990)
5 COOPER, J.A., DEWHURST, R.J., and PALMER, S.B.: 'Characterization of surface-breaking defects in metals with the use of laser-generated ultrasound', *Phil. Trans. R. Soc. Lond. A.*, 1986, **320**, pp. 319–328

Referencing technique for intensity-based sensors using fibre optic Bragg gratings

P.M. Cavaleiro, A.B. Lobo Ribeiro and J.L. Santos

Indexing terms: Fibre optic sensors, Gratings in fibres

An all-optical fibre referencing scheme for intensity based sensors which uses two identical fibre Bragg gratings is described. It provides a general and simple miniature sensor design with referencing effectiveness against system power fluctuations. The concept is demonstrated for a reflective-type displacement sensing cavity, and its potential for simultaneous measurand and temperature evaluation is evaluated.

Fibre optic intensity sensors are inherently simple, reliable, versatile and require only a modest amount of interface electronics. An intensity-modulated optical fibre sensor system, intended for accu-

rate measurement applications, must incorporate a referencing mechanism to safeguard against the likely performance degradation of the optical components with ageing and with changes in the environmental conditions [1]. Thus, a reference signal must be provided which can be calibrated out of the sensor response, but which undergoes all the other losses in the system. Several ways to overcome this problem such as the time flight method [2], Q-modulation [3] and multiwavelength techniques [4, 5] have been demonstrated. Each of them has its own relative advantages and disadvantages but, in general, they suffer from several drawbacks, the most relevant being the limited referencing efficiency and significant system complexity (which, in some way, counteract the inherent simplicity and cost effectiveness of intensity based fibre optic sensors).

In this Letter we describe a simple and reliable referencing scheme which works for all types of reflective intensity based fibre optic sensors.

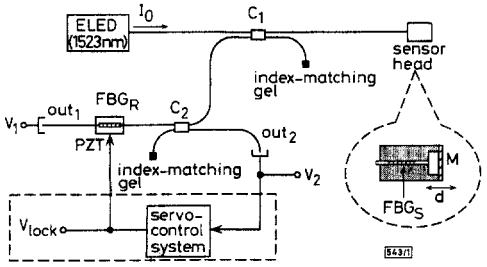

Fig. 1 *Experimental setup of referencing concept*

M: mirror diaphragm, C: directional coupler, FBG: fibre Bragg grating, ELED: edge-light emitting diode, PZT: piezoelectric actuator

The system configuration is shown in Fig. 1 where the intensity sensor is designed as a reflective cavity for primary displacement measurement. It uses two identical fibre Bragg gratings (FBG), one in the sensor head and the other in the processing region. The grating in the sensor head (FBG$_S$) is located just before the exit face to the sensing cavity of the lead fibre. The optical power at the Bragg wavelength (BW) is reflected by the grating and it provides the referencing signal. All the other input spectral power is transmitted by the grating, its power being modulated by the sensor. More precisely, for the case shown in Fig. 1, a fraction $S(d)$ of the excited power is reinjected again in the lead fibre after reflection in the mirror at a distance d. The discrimination of the sensing and referencing optical powers is performed in wavelength by using a second FBG as indicated in Fig. 1. When this grating (FBG$_R$) is prestrained in such a way that the two BWs of the gratings coincide, then the ratio between the signals V_1 and V_2 (the sensing and referencing signals, respectively) gives

$$\frac{V_1}{V_2} = \frac{G}{k_2\alpha_2(1-G)}S(d) \qquad (1)$$

where G is the transmissivity of the gratings, and k_2 and $1-\alpha_2$ the coupling ratio and the power loss factor of the directional coupler C_2, respectively. Clearly, the above ratio is independent of the optical power I_0 injected into the input fibre, as well as of any power fluctuations along the common path of the sensing and referencing signals. The dependence on G is not serious because it has been demonstrated that, for fixed conditions, the transmissivity of the fibre gratings is remarkably stable after some hours from the manufacturing period [6]. On the other hand, coupler C_2 can be placed in a controlled environment in the processing region, allowing a high degree of stability for parameters k_2 and α_2. Therefore, as it should be, the ratio V_1/V_2 depends only on $S(d)$, i.e. the transfer function on the sensor head.

It is important to realise that the BW of the grating FBG$_S$ changes with corresponding variations of several physical measurands, particularly temperature. The temperature sensitivity of the FBGs is typically 13pm/°C around 1.55μm [7]. Therefore, and as an example, for a 30°C temperature variation in the sensor head, the optical reference signal shifts in wavelength by 0.39nm, which means that it becomes detuned from the resonance wavelength of the FBG$_R$. This will degrade the reference signal V_2 to such an extent that correct operation of the proposed concept will not be possible. However, this drawback can be overcome by implementing a servo-control system (dotted box in Fig. 1), which will continually tune the BW of the receiving grating to the BW of the grating in the sensor head [7]. This will not only solve the mentioned problem, but also enable sensor head temperature measurement (the feedback signal V_{lock} in Fig. 1 is directly proportional to the grating temperature in the sensor head). Also, it must be pointed out that temperature variations in the sensor head shift the BW of the gratings relative to the spectrum of the optical source. Because this spectrum is not flat, it will bring some degree of variation in the amplitude of the reference signal V_2. However, this effect can be negleted because the spectral width of LEDs is large (for operation around 1550nm is ~80nm) and the variation in the BW of the gratings is relatively small (as seen before, for 30°C temperature variation, the BW shift is ~0.4nm).

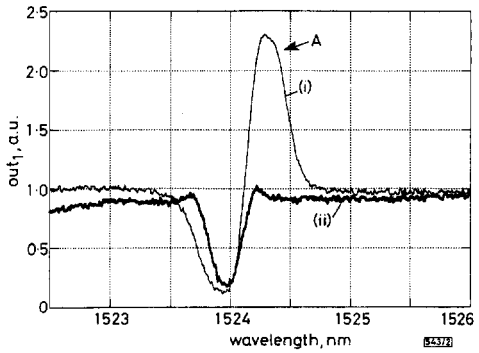

Fig. 2 *Spectra at output 1 when Bragg wavelengths of two gratings are detuned, and tuned to each other*

(I) detuned
(ii) tuned

The presented concept was tested with the configuration shown in Fig. 1. The optical source was a pigtailed ELED (Epitaxx, ETX-1550FJS) with a spectral width of 75nm and spectral peak at 1523nm. The optical power I_0 injected into the system was ~7μW.

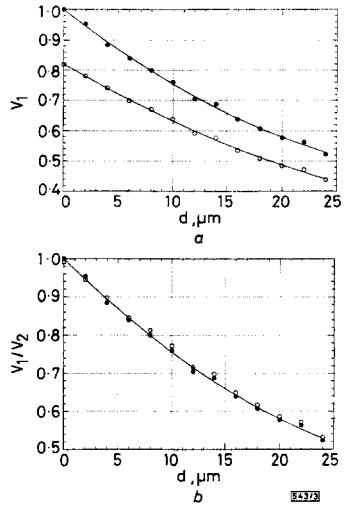

Fig. 3 *Transfer functions of reflective-type displacement sensor without and with referencing*

All data are normalised to value at d = 0μm and I = 100mA
a Without referencing
b With referencing

Two fibre gratings were fabricated with similar characteristics, namely BW of 1524nm (at 25°C), spectral width of ~0.44nm and 90% reflectivity. The sensor head design is detailed in the inset diagram of Fig. 1. Fig. 2 illustrates the effect of tuning the two

fibre Bragg gratings. Curve (i) is the spectrum of the detected signal at output 1 when the two gratings are detuned. The BW of the sensor head grating is not affected by the receiving grating, originating peak A in the spectrum. By applying strain to this grating through the PZT, it is possible to tune the spectra (shown in curve (ii) where it is clear that peak A has disappeared from output 1, being now the reference signal at output 2).

Fig. 3 shows the well known transfer function of the reflective type intensity based sensor. Fig. 3*a* gives the signal V_1 against d, the distance between the exit face of the fibre and the mirror in the sensor head. Two cases are considered, namely the ELED operating with currents of 100 and 80mA (it has been observed that the emitted optical spectrum is very similar for both cases). This means different levels of optical power injected into the system, the consequences of which are clearly seen in Fig. 3*a*. The two scaled curves mean that severe scaling errors in the determination of d will be introduced by a precalibrated sensor of this type, probably invalidating its operation. In contrast, Fig. 3*b* shows the ratio V_1/V_2. As can be seen, the two curves are nearly coincident (the maximum relative deviation does not exceed 1.6%), illustrating the effectiveness of the proposed referencing scheme (even this small deviation can be probably attributed to a non-identical emitted spectrum for the two cases and, also, to the limited accuracy of the processing electronics). It should be emphasised that the referencing technique described above is independent of the structure of the sensor head, the only requirement being that it needs to be of the reflective type.

In conclusion, we have described and demonstrated a new all optical referencing concept for intensity-type fibre optic sensors which is based on the use of two identical fibre Bragg gratings. The potential of the concept for sensing with simultaneous measurand and temperature determination has also been described.

Acknowledgments: The authors wish to thank F.M. Araújo for fabricating the fibre Bragg gratings used in this work. A.B. Lobo Ribeiro ackowledges the financial support of 'Programa PRAXIS XXI'. This work was performed in the framework of the BRITE-EURAM NOSOST project.

1 December 1994

Electronics Letters Online No: 19950244

P.M. Cavaleiro, A.B. Lobo Ribeiro and J.L. Santos (*Grupo de Optoelectrónica, INESC, R. José Falcão 110, 4000 Porto, Portugal*)

J.L. Santos is also with Lab. de Física, Universidade do Porto, Pr. Gomes Teixeira, 4000 Porto, Portugal

References

1 CULSHAW, B., and DAKIN, J.: 'Optical fibre sensors – systems and applications, Vol. II' (Artech House, London, 1989)

2 ADAMOVSKY, G.: 'All-fibre sensing loop using pulse modulated light-emitting diode', *Electron. Lett.*, 1985, **21**, pp. 922–923

3 MACDONALD, R.I., and NYCHKA, R.: 'Differential measurement technique for optical fibre sensors', *Electron. Lett.*, 1991, **27**, pp. 2194–2196

4 MURTAZA, G., and SENIOR, J.: 'Methods for providing stable optical signals in dual wavelength referenced LED based sensors', *IEEE Photonics Technol. Lett.*, 1994, **6**, pp. 1020–1022

5 HE, G., KLUZNER, M., and WLODARCZYK, M.T.: 'Fiber-optic sensor employing thin-film-coating optical spectrum modulation', *Opt. Lett.*, 1993, **18**, pp. 1113–1115

6 ERDOGAN, T., MIZRAHI, V., LEMAIRE, P.J., and MONROE, D.: 'Decay of ultraviolet-induced fiber Bragg gratings', *J. Appl. Phys.*, 1994, **76**, pp. 73–80

7 BRADY, G.P., HOPE, S., LOBO RIBEIRO, A.B., WEBB, D.J., REEKIE, L., ARCHAMBAULT, J.L., and JACKSON, D.A.: 'Demultiplexing of fibre Bragg grating temperature and strain sensors', *Opt. Commun.*, 1994, **111**, pp. 51–54

High-speed SLM with a photosensitive polymer layer

N.V. Kamanina and N.A. Vasilenko

Indexing terms: Spatial light modulators, Photoconducting devices, Liquid crystal devices, Optical polymers

A switch-on time of 3ms and a switch-off time of 20ms have, for the first time, been obtained in spatial light modulators with a photosensitive polymer layer.

It has already been determined that a spatial light modulator (SLM) with a photosensitive polymer layer has high resolution typical of a molecular medium [1, 2]. However, for these devices one of the principal disadvantages is a low speed (switch-on and switch-off times are 20ms and several hundred milliseconds, respectively [3]).

In the present Letter an SLM has been proposed that is several times the speed.

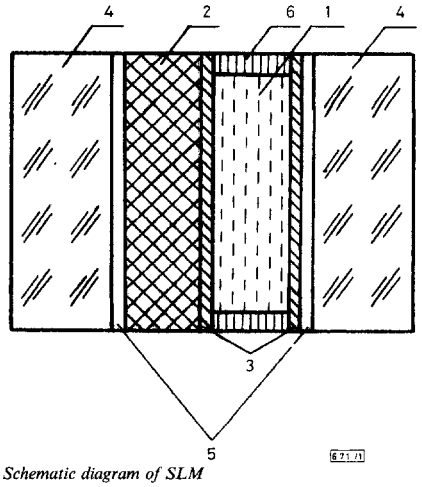

Fig. 1 *Schematic diagram of SLM*

1 liquid crystal
2 photosensitive polymer layer
3 alignment film
4 glass substrates
5 transparent electrodes
6 stoppers

Fig. 1 shows a schematic diagram of the SLM. The photosensitive layer was a thin (1μm) film of sensitised polyimide. Its dark resistivity was $3 \times 10^3 \Omega$cm, whereas its light resistivity was changed by a factor of 100. An electro-optical layer was nematic liquid crystal (LC) with positive dielectric constant anisotropy. Its thickness was 5μm. The initial orientation of the LC was homogeneous.

In the SLM with a photosensitive polymer layer, amorphous carbon film produced by glow plasma [4] was first used as an alignment film. The film thickness was 50nm.

The setup for measuring SLM dynamic characteristics is shown schematically in Fig. 2. The second harmonic (532nm) of the pulse Nd-laser with a pulsewidth of 20ns was used for writing a holographic grating. The diameter of the spot on the photolayer was about 5mm, and the density of the writing power was 4×10^{-4}J/cm^2. The grating was recorded at spatial frequency of 100mm^{-1}.

The readout in a transmission was performed with a CW He-Ne laser (633nm) with a power density of 10^{-4}W/cm^2. The grating vector and readout radiation field vector were aligned with the LC director during writing and readout.

The amplitudes of the rectangular pulses of positive and negative supply voltages were 30V and 10V, respectively. The pulsewidth was 30ms and the repetition frequency was 5Hz. The supply voltage pulses were in synchronism with the laser pulses. A delay between the laser pulse and the front of the supply pulse was 50μs.